1995-05

Horizon irregularity induced by turbulence

Fried, David L.

Horizon irregularity induced by turbulence

David L. Fried

Department of Physics, Naval Postgraduate School, Monterey, California 93943-5000

Received January 25, 1994; revised manuscript received November 3, 1994; accepted November 11, 1994

At any instant the optical effects of atmospheric turbulence can result in a somewhat distorted image. As a consequence, the image of the horizon that ought to appear to be a smooth straight line may instead appear somewhat irregular. When we consider turbulence effects we call into question the idea that a small object that we expect to see just above the horizon will stand out (i..e., will be detectable) because it appears as a bump on what is otherwise a smooth straight horizon line. The degree of irregularity that turbulence may be expected to introduce in the image of the horizon is studied, and a theory that permits evaluation of the vertical irregularity as a function of horizontal extent is developed. It is concluded that for a sample case the effect is small but that, for an object close enough to the horizon line, the detection of this object could be interfered with by this effect.

Key words: turbulence, image distortion, horizon, apparent irregularity, target detection.

1. INTRODUCTION

The research presented here was motivated by an interest in using the nominal smoothness of the line defining the horizon at sea as a way of deciding that a manmade object is visible just above the horizon. The underlying idea is that if such an object is present it will add a small bump to the horizon line, an anomaly whose presence would indicate the existence of the manmade object providing that the horizon line does normally appear to be smooth. But if the horizon line does not generally appear to be smooth, then the bump induced by the manmade object will not be recognized as an anomaly.

In many cases the horizon is nominally smooth (e.g., at sea on a calm day). However, because of atmospheric-turbulence effect, it may be that although the horizon is nominally smooth the image presented to the observer will show the horizon line as irregular. Turbulence effects might cause light originating in the region just below the horizon line to appear to the image-forming system as though it came from a place just above the horizon line, resulting in the apparent irregularity in the image of the horizon line. In this paper our interest is in the development of analytic results that will allow us to assess the magnitude of this effect.

The imaging sensor is considered here to form a spatially quantized focal-plane image, an area-filling array of image pixels. The question is asked, e.g., for an image pixel nominally viewing a region just below (above) the horizon, What is the likelihood that the light reaching that image pixel's region of the focal plane originated above (below) the horizon but, because of turbulence effects, entered the imaging system's optics with the appearance of having come from below (above) the horizon?

To address this matter we might direct our attention to the question of how far away from the nominal source position in the horizon scene the light reaching any image pixel originated. If we knew the rms deviation between the nominal source position and the actual source position for the light reaching any image pixel, then we could calculate the expected irregularity of the image of the horizon. However, it has been found that to address this question directly involves us in an exceptionally complex analysis. An essentially equivalent physical question, which asks where the light from a region in the horizon scene ends up on the image plane (rather than where the light at some position on the image plane came from), has been found to be much more tractable analytically. I have chosen to address the latter issue, arguing from a physical understanding of the situation that the results so obtained are directly applicable to the question of turbulence-induced irregularity of the image of the horizon.

To proceed in this direction we start by considering the horizon scene being viewed as consisting of an array of source pixels nominally corresponding, one to one, to the image pixels. We consider the light from such a source pixel and ask where it falls on the focal plane of our sensor. We want to know, on a rms basis, how far away the centroid of this light is from its nominal position, the focal-plane position at which it would be if there were no turbulence effects, i.e., the position of its nominally corresponding image pixel. The vertical component of this rms displacement is of direct interest to us as it represents the amount that we may expect a nominally straight and horizontal horizon line to move up or down.

However, simple vertical displacement is not necessarily of concern to us. If a large lateral extent of the horizon line (i.e., a region several pixels wide) is vertically displaced, it is highly likely that this displacement would not even be noticed; it is only the vertical displacement of a small portion of the horizon line, e.g., a portion just 1 or 2 pixels wide, that could create the appearance of a manmade object located just above the horizon. To take account of this matter we shall evaluate the mean-square difference of the turbulence-induced vertical displacements of the centroids of the images of a pair of source pixels for various horizontal separations of the source pixels.[1]

0740-3232/95/050950-08$06.00

2. FORMULATION AND DEFINITION OF QUANTITIES

Let us consider the horizontal straight line just discussed as defining the x axis, with the vertical direction defining the y axis. We consider an imaging system with an aperture diameter D and detectors and focal length such as to define a square pixel whose angular subtense is $\alpha \times \alpha$, with each side of the square being parallel to the x axis or to the y axis. We consider this source pixel to be defined in terms of the physical region in the field of view that nominally (i.e., in the absence of turbulence effects) provides the light reaching the image pixel. The turbulence will alter the apparent direction from which the light from the source pixel appears to arrive. To the extent that this direction is altered, we may expect that the actual direction to the source of the light that reaches the actual image pixel is altered. Accordingly, the intention herein is to study the statistics of the turbulence effect on the apparent direction associated with the light from a source pixel. In this paper, when the term pixel is used, it means not a portion of the sensor's focal plane (a portion defined by some detector) but rather the portion of the physical background that nominally corresponds to the focal-plane region that ordinarily is considered to constitute a pixel.

The notation $\boldsymbol{\vartheta}$ is used to denote the true angular position of a point in the background pattern with the x- and the y-axis components of $\boldsymbol{\vartheta}$ being denoted by ϑ_x and ϑ_y, respectively, so that $\boldsymbol{\vartheta} \equiv [\vartheta_x, \vartheta_y]_{\text{rect}}$. As used here, the term true is intended to indicate that the position is determined entirely by geometry and is uninfluenced by randomly varying turbulence effects. The notation $S(\boldsymbol{\vartheta})$ is used to denote the square region in the field of view corresponding to a pixel centered at the origin. This function is defined by the equation

$$S(\boldsymbol{\vartheta}) = \begin{cases} 1, & \text{if } [(|\vartheta_x| \le 1/2\alpha), \quad (|\vartheta_y| \le 1/2\alpha)] \\ 0, & \text{otherwise} \end{cases}. \tag{1}$$

We use the notation $\theta(\boldsymbol{\vartheta})$ to denote the turbulence-induced tilt of the light from a point source whose true direction is $\boldsymbol{\vartheta}$, the tilt that is considered to be only for the portion of the light that enters our sensor aperture. Thus, for a point source located at $\boldsymbol{\vartheta}$, the apparent direction of the point source, as seen by the sensor, will be $\boldsymbol{\vartheta} + \theta(\boldsymbol{\vartheta})$. The quantity $\theta(\boldsymbol{\vartheta})$ is to be understood as a perturbation, the amount by which the apparent direction to the point source deviates from the true direction $\boldsymbol{\vartheta}$. Whereas $\boldsymbol{\vartheta}$ is to be understood as representing a true position in the field of view, with a value that is not influenced by turbulence effects and with a magnitude that is most reasonably measured in degrees (or in radians), the notation $\theta(\boldsymbol{\vartheta})$, which represents the turbulence-induced perturbation of the pixel's apparent position and is a quantity whose value is determined entirely by turbulence effects, has a magnitude that is most reasonably measured in seconds of arc (or in microradians).

The perturbation $\theta(\boldsymbol{\vartheta})$ can be shown to have a mean value of zero, which implies that both the x and the y components, i.e., θ_x and θ_y, have mean values equal to zero. We are interested only in the y component θ_y. The second moment of θ_y is most usefully presented, for our purposes, in terms of its structure function. The structure function is defined by the equation

$$\mathcal{D}_{\theta_y}(\boldsymbol{\vartheta}) = \langle |\theta_y(\boldsymbol{\vartheta}' + 1/2\boldsymbol{\vartheta}) - \theta_y(\boldsymbol{\vartheta}' - 1/2\boldsymbol{\vartheta})|^2 \rangle. \tag{2}$$

The turbulence-induced tilt $\boldsymbol{\Theta}$ for some source pixel is equal to the average of the point-source tilt θ, with the average being taken over all the point sources constituting the source pixel. For the pixel centered in the direction $\boldsymbol{\vartheta}$, the pixel's tilt $\boldsymbol{\Theta}(\boldsymbol{\vartheta})$ has a value given by the equation

$$\boldsymbol{\Theta}(\boldsymbol{\vartheta}) \equiv \alpha^{-2} \int \mathrm{d}\boldsymbol{\vartheta}' S(\boldsymbol{\vartheta}' - \boldsymbol{\vartheta}) \boldsymbol{\theta}(\boldsymbol{\vartheta}'). \tag{3}$$

Our interest is in the y component of $\boldsymbol{\Theta}(\boldsymbol{\vartheta})$, i.e., in $\Theta_y(\boldsymbol{\vartheta})$. By changing the variable of integration and restricting our attention to the vertical displacement, we obtain

$$\Theta_y(\boldsymbol{\vartheta}) = \alpha^{-2} \int \mathrm{d}\vartheta' S(\boldsymbol{\vartheta}') \theta_y(\boldsymbol{\vartheta}' + \boldsymbol{\vartheta}). \tag{4}$$

The measure of the effect in which we are interested is the structure function for the y component of the turbulence-induced pixel displacement when the separation between pixels has only an x component. This structure function is denoted by $\mathcal{D}_{\Theta_y}([\vartheta_x, 0]_{\text{rect}})$ and defined by the equation

$$\begin{aligned} \mathcal{D}_{\Theta_y}([\vartheta_x, 0]_{\text{rect}}) \equiv \langle |\Theta_y(\vartheta' + 1/2[\vartheta_x, 0]_{\text{rect}}) \\ - \Theta_y(\vartheta' - 1/2[\vartheta_x, 0]_{\text{rect}})|^2 \rangle. \end{aligned} \tag{5}$$

The basic problem is the development of numerical results for this expression. As can be seen, it provides a direct measure of the vertical irregularity of the image of what should be a horizontal straight line. We start accomplishing this task with a reformulation of the problem.

3. REFORMULATION

Substituting Eq. (4) into Eq. (5), making an integral of the difference of integrands out of the difference of integrals, expressing the square of the integral as the product of the integral with itself, and then making a double integral of the product of integrals, we obtain a result that can be written as

$$\begin{aligned} \mathcal{D}_{\Theta_y}([\vartheta_x, 0]_{\text{rect}}) = \alpha^{-4} \iint \mathrm{d}\boldsymbol{\vartheta}'' \mathrm{d}\boldsymbol{\vartheta}''' S(\boldsymbol{\vartheta}'') S(\boldsymbol{\vartheta}''') \\ \times \langle \{\theta_y(\boldsymbol{\vartheta}'' + \boldsymbol{\vartheta}' + 1/2[\vartheta_x, 0]_{\text{rect}}) \\ - \theta_y(\boldsymbol{\vartheta}'' + \boldsymbol{\vartheta}' - 1/2[\vartheta_x, 0]_{\text{rect}})\} \\ \times \{\theta_y(\boldsymbol{\vartheta}''' + \boldsymbol{\vartheta}' + 1/2[\vartheta_x, 0]_{\text{rect}}) \\ - \theta_y(\boldsymbol{\vartheta}''' + \boldsymbol{\vartheta}' - 1/2[\vartheta_x, 0]_{\text{rect}})\} \rangle. \end{aligned} \tag{6}$$

Making use of the fact that

$$\begin{aligned} (a - b)(c - d) = 1/2[-(a - c)^2 - (b - d)^2 \\ + (a - d)^2 + (b - c)^2] \end{aligned} \tag{7}$$

and utilizing Eq. (2), we can recast Eq. (6) as

$$\mathcal{D}_{\Theta_y}([\vartheta_x, 0]_{\rm rect}) = \frac{1}{2}\alpha^{-4}\iint \mathrm{d}\boldsymbol{\vartheta}''\mathrm{d}\boldsymbol{\vartheta}'''S(\boldsymbol{\vartheta}'')S(\boldsymbol{\vartheta}''')$$
$$\times \{\langle|\theta_y(\boldsymbol{\vartheta}'' + \boldsymbol{\vartheta}' + 1/2[\vartheta_x, 0]_{\rm rect})$$
$$- \theta_y(\boldsymbol{\vartheta}''' + \boldsymbol{\vartheta}' + 1/2[\vartheta_x, 0]_{\rm rect})|^2\rangle$$
$$- \langle|\theta_y(\boldsymbol{\vartheta}'' + \boldsymbol{\vartheta}' - 1/2[\vartheta_x, 0]_{\rm rect})$$
$$- \theta_y(\boldsymbol{\vartheta}''' + \boldsymbol{\vartheta}' - 1/2[\vartheta_x, 0]_{\rm rect})|^2\rangle$$
$$+ \langle|\theta_y(\boldsymbol{\vartheta}'' + \boldsymbol{\vartheta}' + 1/2[\vartheta_x, 0]_{\rm rect})$$
$$- \theta_y(\boldsymbol{\vartheta}''' + \boldsymbol{\vartheta}' - 1/2[\vartheta_x, 0]_{\rm rect})|^2\rangle$$
$$+ \langle|\theta_y(\boldsymbol{\vartheta}'' + \boldsymbol{\vartheta}' - 1/2[\vartheta_x, 0]_{\rm rect})$$
$$- \theta_y(\boldsymbol{\vartheta}''' + \boldsymbol{\vartheta}' + 1/2[\vartheta_x, 0]_{\rm rect})|^2\rangle\}$$
$$= \frac{1}{2}\alpha^{-4}\iint \mathrm{d}\boldsymbol{\vartheta}''\mathrm{d}\boldsymbol{\vartheta}'''S(\boldsymbol{\vartheta}'')S(\boldsymbol{\vartheta}''')$$
$$\times \{\mathcal{D}_{\theta_y}(\boldsymbol{\vartheta}'' - \boldsymbol{\vartheta}''' + [\vartheta_x, 0]_{\rm rect})$$
$$+ \mathcal{D}_{\theta_y}(\boldsymbol{\vartheta}'' - \boldsymbol{\vartheta}''' - [\vartheta_x, 0]_{\rm rect})$$
$$- 2\mathcal{D}_{\theta_y}(\boldsymbol{\vartheta}'' - \boldsymbol{\vartheta}''')\}. \quad (8)$$

We can significantly simplify this expression by changing the variables of integration to the sum and the difference variables, namely, $\boldsymbol{\vartheta}_+ = (1/2)(\boldsymbol{\vartheta}'' + \boldsymbol{\vartheta}''')$ and $\boldsymbol{\vartheta}_- = \boldsymbol{\vartheta}'' - \boldsymbol{\vartheta}'''$. This allows us to rewrite Eq. (8) as

$$\mathcal{D}_{\Theta_y}([\vartheta_x, 0]_{\rm rect}) = \frac{1}{2}\alpha^{-2}\int \mathrm{d}\boldsymbol{\vartheta}_- S(\boldsymbol{\vartheta}_-)$$
$$\times \{\mathcal{D}_{\theta_y}(\boldsymbol{\vartheta}_- + [\vartheta_x, 0]_{\rm rect})$$
$$+ \mathcal{D}_{\theta_y}(\boldsymbol{\vartheta}_- - [\vartheta_x, 0]_{\rm rect})$$
$$- 2\mathcal{D}_{\theta_y}(\boldsymbol{\vartheta}_-)\}, \quad (9)$$

where the quantity $S(\boldsymbol{\vartheta}_-)$ is defined by the equation

$$S(\boldsymbol{\vartheta}_-) \equiv \alpha^{-2}\int \mathrm{d}\boldsymbol{\vartheta}_+ S(\boldsymbol{\vartheta}_+ + 1/2\boldsymbol{\vartheta}_-)S(\boldsymbol{\vartheta}_+ - 1/2\boldsymbol{\vartheta}_-). \quad (10)$$

It is easy to see that, with the pixel having a square shaper with sides of length α, we have

$$S(\boldsymbol{\vartheta}) = \begin{cases} (1 - |\vartheta_x|/\alpha)(1 - |\vartheta_y|/\alpha) & \text{if } [(|\vartheta_x| \le \alpha), (|\vartheta_y| \le \alpha)] \\ 0 & \text{otherwise} \end{cases}. \quad (11)$$

By virtue of the invariance of $S(\vartheta)$ on a change of sign of ϑ and of the invariance of $\mathcal{D}_{\theta_y}(\vartheta)$ under this same change of sign, we see that Eq. (9) can be recast in the form

$$\mathcal{D}_{\theta_y}([\vartheta_x, 0]_{\rm rect}) = \alpha^{-2}\int \mathrm{d}\boldsymbol{\vartheta}' S(\boldsymbol{\vartheta}')$$
$$\times \{\mathcal{D}_{\theta_y}(\boldsymbol{\vartheta}' + [\vartheta_x, 0]_{\rm rect}) - \mathcal{D}_{\theta_y}(\boldsymbol{\vartheta}')\}. \quad (12)$$

To proceed beyond this point we need a numerically tractable expression for $\mathcal{D}_{\theta_y}(\boldsymbol{\vartheta})$. This is presented in Section 4.

4. POINT-SOURCE SEPARATION VARIATION STATISTICS

In another study[2] the statistics of the turbulence-induced variation of the apparent separation of a pair of point sources were examined. In that work it was shown that the quantity denoted there by C_{yy}, which corresponds to the structure function $\mathcal{D}_{\theta_y}(\boldsymbol{\vartheta})$, i.e.,

$$\mathcal{D}_{\theta_y}(\boldsymbol{\vartheta}) = C_{yy}, \quad (13)$$

has a value such that

$$\mathcal{D}_{\theta_y}(\boldsymbol{\vartheta}) = C_0(\boldsymbol{\vartheta}) - C_2(\boldsymbol{\vartheta})\cos(2\phi), \quad (14)$$

where ϕ is the angle between the x axis and the separation vector $\boldsymbol{\vartheta}$. Inasmuch as $\cos(2\phi) = \cos^2(\phi) - \sin^2(\phi)$ with $\cos(\phi) = \vartheta_x(\vartheta_x{}^2 + \vartheta_y{}^2)^{-1/2}$ and $\sin(\phi) = \vartheta_y(\vartheta_x{}^2 + \vartheta_y{}^2)^{-1/2}$, then we can write

$$\cos(2\phi) = \frac{\vartheta_x{}^2 - \vartheta_y{}^2}{\vartheta_x{}^2 + \vartheta_y{}^2}. \quad (15)$$

Thus we can rewrite Eq. (14) as

$$\mathcal{D}_{\theta_y}(\boldsymbol{\vartheta}) = C_0(\boldsymbol{\vartheta}) - C_2(\boldsymbol{\vartheta})\frac{\vartheta_x{}^2 - \vartheta_y{}^2}{\vartheta_x{}^2 + \vartheta_y{}^2}. \quad (16)$$

The quantities $C_0(\boldsymbol{\vartheta})$ and $C_2(\boldsymbol{\vartheta})$ have values given by the expressions

$$C_0(\boldsymbol{\vartheta}) = 2.91\frac{128}{\pi^2}SD^{-1/3}\int_0^1 \mathrm{d}\eta C_N^2(\eta S)\int_0^1 z\mathrm{d}z$$
$$\times [\cos^{-1}(z) - z(3 - 2z^2)\sqrt{1 - z^2}]$$
$$\times \left(2\pi z^{5/3}(1 - \eta)^{5/3}\left\{J_0\left[\frac{z(1 - \eta)}{|\boldsymbol{\vartheta}|\eta}\frac{D}{S}\right] - 1\right\}\right), \quad (17)$$

$$C_2(\boldsymbol{\vartheta}) = -2.91\frac{128}{(3/4)\pi^2}SD^{-1/3}\int_0^1 \mathrm{d}\eta C_N^2(\eta S)\int_0^1 z\mathrm{d}z$$
$$\times [-z(1 - z^2)^{3/2}]$$
$$\times \left\{2\pi z^{5/3}(1 - \eta)^{5/3}J_2\left[\frac{z(1 - \eta)}{|\boldsymbol{\vartheta}|\eta}\frac{D}{S}\right]\right\}. \quad (18)$$

Here the quantity S denotes the total propagation path length, and C_N^2 denotes the refractive-index structure constant, which represents the optical strength of turbulence a distance s from the aperture of our imaging system.

The functions $J_0(z)$ and $J_2(x)$ are defined by the equations

$$J_0(z) = \begin{cases} J_0(z)z^{-5/6} & \text{if } z \le 1 \\ J_0(z^{-1})z^{-5/6} & \text{if } z > 1 \end{cases}, \quad (19)$$

$$J_2(z) = \begin{cases} J_2(z)z^{-5/6} & \text{if } z \le 1 \\ J_2(z^{-1})z^{-5/6} & \text{if } z > 1 \end{cases}, \quad (20)$$

where

$$J_0(z) = z^{-5/6}\sum_{k=0}^{\infty}\left[\frac{\Gamma(k - 5/6)}{\Gamma(k + 1)\Gamma(-5/6)}\right]^2 z^{2k}, \quad (21)$$

$$J_2(z) = z^{7/6}\sum_{k=0}^{\infty}\frac{\Gamma(k - 5/6)\Gamma(k + 7/6)}{\Gamma(k + 1)\Gamma(k + 3)[\Gamma(-5/6)]^2}z^{2k}. \quad (22)$$

We recast Eqs. (17) and (18) in the form

$$C_0(\boldsymbol{\vartheta}) = 2.91\,\frac{128}{\pi^2}\,SD^{-1/3}\int_0^1 \mathrm{d}\eta C_N^2(\eta S)\int_0^1 z\mathrm{d}z \times [\cos^{-1}(z) - z(3-2z^2)\sqrt{1-z^2}\,)] \times \left\{2\pi z^{5/3}(1-\eta)^{5/3}\left[J_0\left(z\,\frac{1-\eta}{\eta}\,\frac{1}{|\boldsymbol{\vartheta}|/\alpha}\,Q\right)-1\right]\right\}, \quad (23)$$

$$C_2(\boldsymbol{\vartheta}) = -2.91\,\frac{128}{(3/4)\pi^2}\,SD^{-1/3}\int_0^1 \mathrm{d}\eta C_N^2(\eta S)\int_0^1 z\mathrm{d}z \times [-z(1-z^2)^{3/2}] \times \left[2\pi z^{5/3}(1-\eta)^{5/3}J_2\left(z\,\frac{1-\eta}{\eta}\,\frac{1}{|\boldsymbol{\vartheta}|/\alpha}\,Q\right)\right], \quad (24)$$

where

$$Q = \frac{D}{S\alpha}\,. \quad (25)$$

Because

$$\int_0^1 z\mathrm{d}z[\cos^{-1}(z) - z(3-2z^2)\sqrt{1-z^2}\,] = 0\,, \quad (26)$$

we can recast Eq. (23) as

$$C_0(\boldsymbol{\vartheta}) = 2.91\,\frac{128}{\pi^2}\,SD^{-1/3}\int_0^1 \mathrm{d}\eta C_N^2(\eta S)\int_0^1 z\mathrm{d}z \times [\cos^{-1}(z) - z(3-2z^2)\sqrt{1-z^2}\,] \times \left\{2\pi z^{5/3}(1-\eta)^{5/3}\left[\tilde{J}_0\left(z\,\frac{1-\eta}{\eta}\,\frac{1}{|\boldsymbol{\vartheta}|/\alpha}\,Q\right)-1\right]\right\}, \quad (27)$$

where

$$\tilde{J}_0(z) = J_0(z) - z^{-5/3}\,. \quad (28)$$

Making use of Eqs. (19) and (21) along with Eq. (28), we can write

$$\tilde{J}_0(z) = \begin{cases} z^{-5/3}\displaystyle\sum_{k=1}^{\infty}\left[\frac{\Gamma(k-5/6)}{\Gamma(k+1)\Gamma(-5/6)}\right]^2 z^{2k} & \text{if } z \le 1 \\ 1 - z^{-5/3} + \displaystyle\sum_{k=1}^{\infty}\left[\frac{\Gamma(k-5/6)}{\Gamma(k+1)\Gamma(-5/6)}\right]^2 z^{-2k} & \text{if } z > 1 \end{cases}. \quad (29)$$

It is obvious from inspection that for very large values of z the asymptotic value is $\tilde{J}_0(x) \asymp 1$, whereas for very small values of z the asymptotic value is $\tilde{J}_0(z) \asymp z^{1/3}$. Making use of Eqs. (20) and (22), we can write that

$$J_2(z) = \begin{cases} z^{-5/3}\displaystyle\sum_{k=1}^{\infty}\frac{\Gamma(k-11/6)\Gamma(k+1/6)}{\Gamma(k)\Gamma(k+2)[\Gamma(-5/6)]^2}z^{2k} & \text{if } z \le 1 \\ \displaystyle\sum_{k=1}^{\infty}\frac{\Gamma(k-11/6)\Gamma(k+1/6)}{\Gamma(k)\Gamma(k+2)[\Gamma(-5/6)]^2}z^{-2k} & \text{if } z > 1 \end{cases}. \quad (30)$$

It is obvious from inspection that for very large values of z the asymptotic value is $J_2(z) \asymp -(5/72)z^{-2}$, whereas for very small values of z the asymptotic value is $J_2(z) \asymp -(5/72)z^{1/3}$. Figure 1 shows a plot of $\tilde{J}_0(z)$ and of $-J_2(z)$ versus z.

Returning to the matter of developing a suitable expression for the evaluation of the point-source separation variability structure function $\mathcal{D}_{\theta_y}(\boldsymbol{\vartheta})$, we substitute Eqs. (24) and (27) into Eq. (16) and after suitable rearrangement of the terms obtain

$$C_{\theta_y}(\boldsymbol{\vartheta}) = 2.91\,\frac{256}{\pi}\,SD^{-1/3}\int_0^1 \mathrm{d}\eta(1-\eta)^{5/3}C_N^2(\eta S) \times \int_0^1 \mathrm{d}z z^{8/3}\left\{[\cos^{-1}(z) - z(3-2z^2)\sqrt{1-z^2}\,] \times \left[\tilde{J}_0\left(z\,\frac{1-\eta}{\eta}\,\frac{1}{|\boldsymbol{\vartheta}|/\alpha}\,Q\right)-1\right] - [z(1-z^2)^{3/2}]J_2\left(z\,\frac{1-\eta}{\eta}\,\frac{1}{|\boldsymbol{\vartheta}|/\alpha}\,Q\right)\left(\frac{{\theta_x}^2-{\theta_y}^2}{{\theta_x}^2+{\theta_y}^2}\right)\right\}. \quad (31)$$

Inasmuch as no further analytic reduction appears to be possible, we consider Eq. (31) to provide the basis for the numerical evaluation of the point-source separation variability structure function $\mathcal{D}_{\theta_y}(\boldsymbol{\vartheta})$. We are now ready to take up the matter of the numerical evaluation of the source-pixel separation variability structure function $\mathcal{D}_{\theta_y}([\vartheta_x, 0]_{\mathrm{rect}})$. This subject is treated in Section 5.

5. PIXEL SEPARATION VARIATION STATISTICS

Starting with Eq. (12), substituting Eq. (31), making use of Eq. (11), and changing the variable of integration from

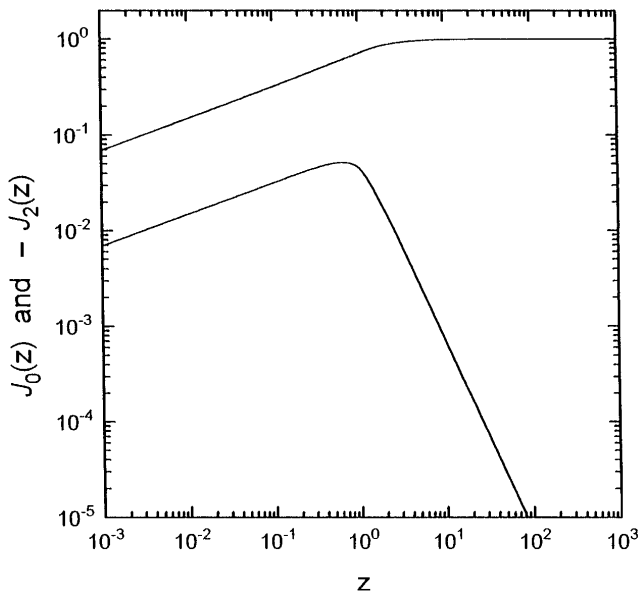

Fig. 1. $\tilde{J}_0(z)$ and $-J_2(z)$ versus z. We calculate the results shown here using Eqs. (29) and (30), summing the power series through the first 25 terms. The upper curve is for $\tilde{J}_0(z)$. This curve is asymptotic to $(25/36)z^{1/3}$ for very small values of z and to $1 - z^{-5/6} + (25/36)z^{-2}$ for very large values of z. The lower curve is for $-J_2(z)$. This curve is asymptotic to $-(5/72)z^{1/3}$ for very small values of z and to $-(5/72)z^{-2}$ for very large values of z.

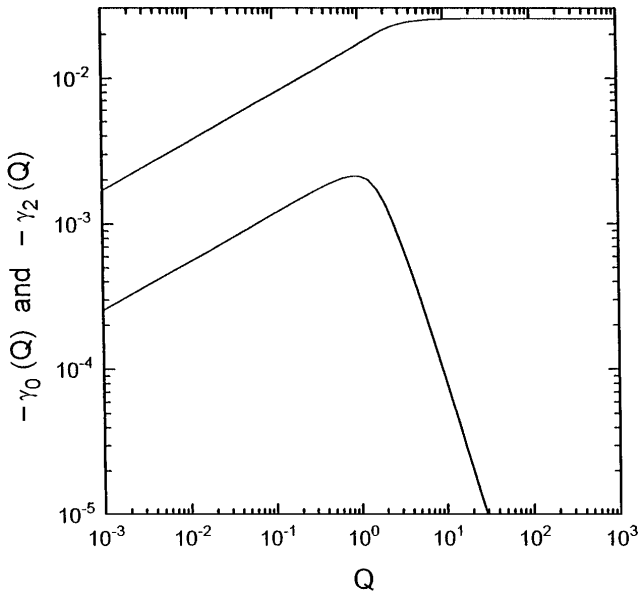

Fig. 2. $-\gamma_0(Q)$ and $-\gamma_2(Q)$ versus Q. The results shown here are calculated by using Eq. (35) for $-\gamma_0(Q)$ and Eq. (36) for $-\gamma_2(Q)$. The curves appear to have the same asymptotic behavior as the curves shown in Fig. 1.

$\boldsymbol{\vartheta}'$ to $\boldsymbol{\nu} = [\nu_x, \nu_y]_{\text{rect}}$, where $[\nu_x, \nu_y] \equiv \boldsymbol{\vartheta}'/\alpha$, we can write

$$\mathcal{D}_{\theta_y}([n_x, \alpha, 0]_{\text{rect}}) = 2.91 \frac{256}{\pi} SD^{-1/3} \int_{-1}^{1}\int_{-1}^{1} d\nu_x d\nu_y \times (1 - |\nu_x|)(1 - |\nu_y|) \int_0^1 d\eta (1-\eta)^{5/3} C_N^2(\eta S) \times \int_0^1 dz z^{8/3} \Bigg[[\cos^{-1}(z) - z(3 - 2z^2)(1 - z^2)^{1/2}] \times \Bigg(\tilde{J}_0\left\{ z \frac{1-\eta}{\eta} \frac{1}{[(\nu_x + n_x)^2 + \nu_y^2]^{1/2}} Q \right\} - \tilde{J}_0\left[z \frac{1-\eta}{\eta} \frac{1}{(\nu_x^2 + \nu_y^2)^{1/2}} Q \right] \Bigg) - [z(1 - z^2)^{3/2}] \times \Bigg(J_2\left\{ z \frac{1-\eta}{\eta} \frac{1}{[(\nu_x + n_x)^2 + \nu_y^2]^{1/2}} Q \right\} \times \left[\frac{(\nu_x + n_x)^2 - \nu_y^2}{(\nu_x + n_x)^2 + \nu_y^2} \right] - J_2\left[z \frac{1-\eta}{\eta} \frac{1}{(\nu_x^2 + \nu_y^2)^{1/2}} Q \right] \left(\frac{\nu_x^2 - \nu_y^2}{\nu_x^2 + \nu_y^2} \right) \Bigg) \Bigg]. \quad (32)$$

The quantity n_x corresponds to $n_x \equiv \vartheta_x/\alpha$ and represents the separation of the centers of the two pixels, with the separation being measured in units of the pixel width α.

Put in the form shown in Eq. (32), the evaluation of the structure function $\mathcal{D}_{\theta_y}([n_x, 0]_{\text{rect}})$ represents a straightforward, although somewhat sizable, matter of numerical evaluation. To simplify the numerical treatment of the problem it is helpful to introduce the function $f(n, Q)$, which is defined by the equation

$$f(n, Q) = \int_{-1}^{1}\int_{-1}^{1} d\nu_x d\nu_y (1 - |\nu_x|)(1 - |\nu_y|) \times \int_0^1 dz z^{8/3} \Bigg[[\cos^{-1}(z) - z(3 - 2z^2)(1 - z^2)^{1/2}] \times \Bigg(\tilde{J}_0\left\{ z \frac{1}{[(\nu_x + n)^2 + \nu_y^2]^{1/2}} Q \right\} - \tilde{J}_0\left[z \frac{1}{(\nu_x^2 + \nu_y^2)^{1/2}} Q \right] \Bigg) - [z(1 - z^2)^{3/2}] \times \Bigg(J_2\left\{ z \frac{1}{[(\nu_x + n)^2 + \nu_y^2]^{1/2}} Q \right\} \times \left[\frac{(\nu_x + n)^2 - \nu_y^2}{(\nu_x + n)^2 + \nu_y^2} \right] - J_2\left[z \frac{1}{(\nu_x^2 + \nu_y^2)^{1/2}} Q \right] \left(\frac{\nu_x^2 - \nu_y^2}{\nu_x^2 + \nu_y^2} \right) \Bigg) \Bigg]. \quad (33)$$

Making use of this function, we can rewrite Eq. (32) as

$$\mathcal{D}_{\Theta_y}([n_x\alpha, 0]_{\text{rect}}) = 2.91 \frac{256}{\pi} SD^{-1/3} \int_0^1 d\eta (1-\eta)^{5/3} \times C_N^2(\eta S) f\left(n_x, \frac{1-\eta}{\eta} \frac{D}{S\alpha} \right). \quad (34)$$

The basic computational task can now be seen to be that of evaluating $f(n, Q)$. We can simplify this task by defining the functions $\gamma_0(Q)$ and $\gamma_2(Q)$ according to the

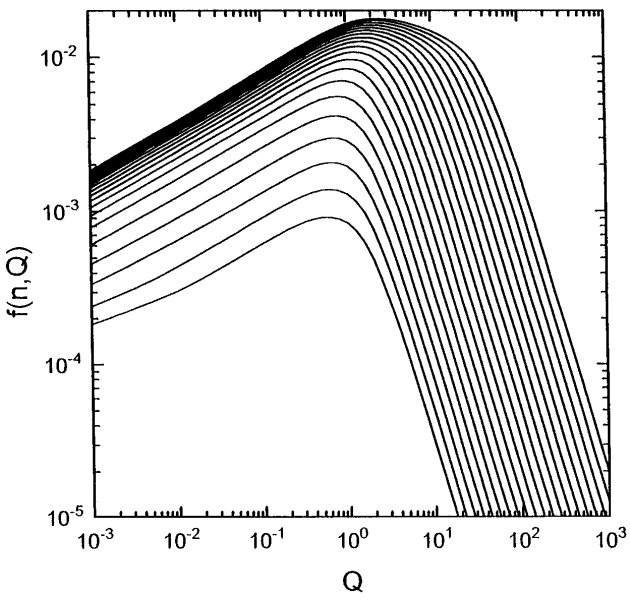

Fig. 3. $f(n, Q)$ versus Q. The results shown here are calculated by using Eqs. (37)–(39). The 20 separate curves correspond to 20 distinct values of n. The values of n are uniformly spaced in a logarithmic sense, spanning the range from $n = 10^{-0.5}$ to $n = 10^{1.4}$, inclusive. The lower curves correspond to the smaller values of n.

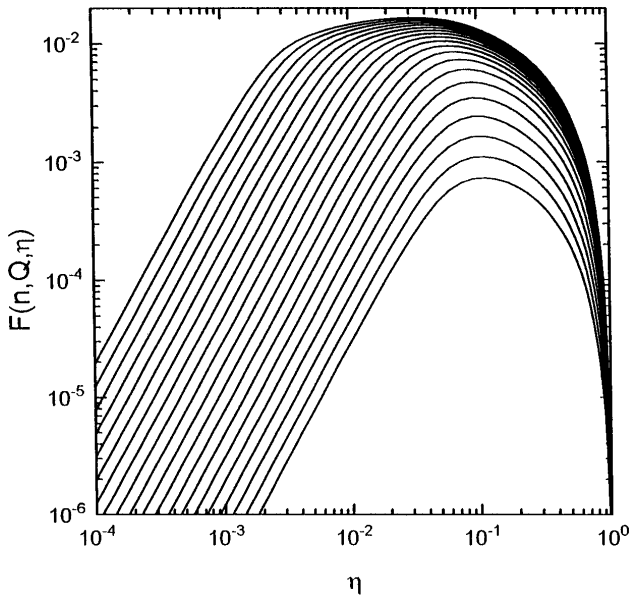

(a)

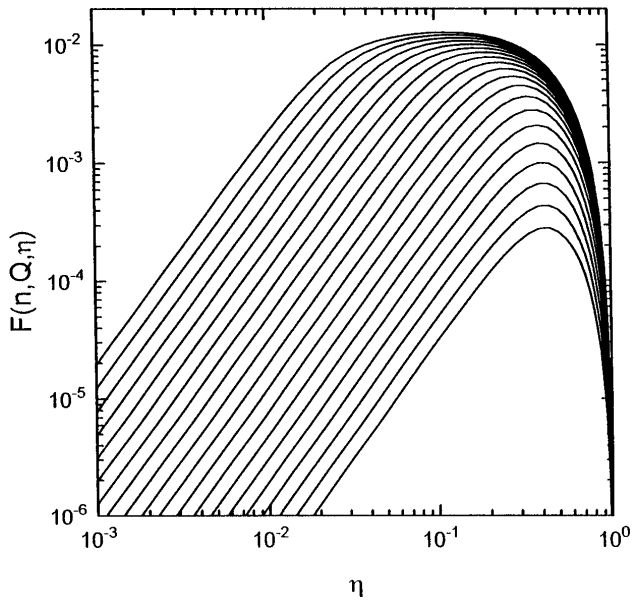

(b)

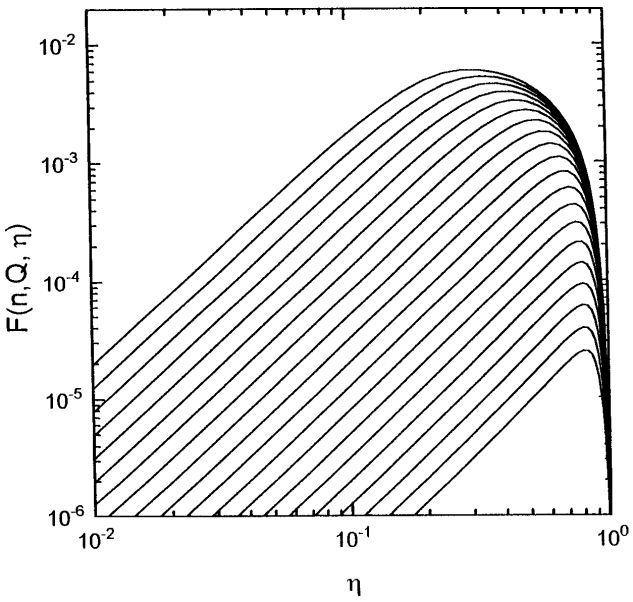

(c)

Fig. 4. $F(n, Q, \eta)$ versus η. (a), (b), and (c) show results for $Q = D/(S\alpha) = 0.1, 1.0, 10.0$, respectively. The 20 curves in each figure correspond to $n = 10^{-1.5}, 10^{-1.4}, 10^{-1.3}, \ldots, 10^{1.3}, 10^{1.4}$, with the lower curves corresponding to the smaller value of n.

equations

$$\gamma_0(Q) = \int_0^1 \mathrm{d}z z^{8/3}[\cos^{-1}(z) - z(3 - 2z^2)\sqrt{1 - z^2}]\tilde{J}_0(zQ), \tag{35}$$

$$\gamma_2(Q) = \int_0^1 \mathrm{d}z z^{11/3}(1 - z^2)^{3/2} J_2(zQ). \tag{36}$$

These two functions (or rather their negatives) are shown in Fig. 2. With these expressions we can write in place of Eq. (33) that

$$f(n, Q) = f_0(n, Q) - f_2(n, Q), \tag{37}$$

where

$$f_0(n, Q) = \int_{-1}^1 \int_{-1}^1 \mathrm{d}x\mathrm{d}y(1 - |x|)(1 - |y|) \times \left(\gamma_0\left\{ \frac{Q}{[(x + n)^2 + y^2]^{1/2}} \right\} - \gamma_0\left[\frac{Q}{(x^2 + y^2)^{1/2}} \right] \right), \tag{38}$$

$$f_2(n, Q) = \int_{-1}^1 \int_{-1}^1 \mathrm{d}x\mathrm{d}y(1 - |x|)(1 - |y|) \times \left(\gamma_2\left\{ \frac{Q}{[(x + n)^2 + y^2]^{1/2}} \right\} \frac{(x + n)^2 - y^2}{(x + n)^2 + y^2} - \gamma_2\left[\frac{Q}{(x^2 + y^2)^{1/2}} \right] \frac{x^2 - y^2}{x^2 + y^2} \right). \tag{39}$$

Figure 3 shows the calculated results for $f(n, Q)$ as a function of Q for 20 values of n that are uniformly spaced in a logarithmic sense to span the range from $n = 10^{-0.5}$ to $n = 10^{1.4}$, inclusive. The lower-lying curves are for the smaller values of n. (The value of n corresponds to the center-to-center separation of pixels, measured in units of the pixel width α.)

It is more interesting to consider this function in the form in which it appears in Eq. (34), examining the dependence on η, because η is used there to represent the normalized distance from the imaging system (we accomplish normalization of the distance by dividing by the range S to the source pixel). In fact, the most useful insight as to dependence on position along the propagation path is provided by rewriting Eq. (34) as

$$\mathcal{D}_{\Theta_y}([n_x\alpha, 0]_{\text{rect}}) = 2.91\frac{256}{\pi}SD^{-1/3}\int_0^1 \mathrm{d}\eta C_N^2(\eta S) \times F\left(n_x, \frac{D}{S\alpha}, \eta\right), \tag{40}$$

where

$$F(n, Q, \eta) = (1-\eta)^{5/3} f\left(n, \frac{1-\eta}{\eta}Q\right), \tag{41}$$

and studying the η dependence of $F(n, Q, \eta)$. Figure 4 shows $F(n, Q, \eta)$ as a function of η for the same 20 values of n that were considered for Fig. 3. Figures 4(a), 4(b), and 4(c) correspond to $Q = D/(S\alpha) = 0.1$, 1.0, 10.0, respectively, i.e., to the aperture diameter equal to 0.1, 1.0, and 10.0 times the linear size of the source pixel. In each of these figures the lower curves correspond to the smaller values of n.

To develop a physically meaningful and quantitative understanding of the implication of these results it is useful to consider Eq. (40) for the case in which $C_N^2(\eta S)$ is a constant over the propagation path, i.e., does not depend on η. In this case we can write

$$\mathcal{D}_{\Theta_y}([n_x\alpha, 0]_{\text{rect}}) = 2.91\frac{256}{\pi}SD^{-1/3}C_N^2 G\left(n_x, \frac{D}{S\alpha}\right), \tag{42}$$

where

$$G(n, Q) = \int_0^1 \mathrm{d}\eta F(n, Q, \eta). \tag{43}$$

This quantity, $G(n, Q)$, is of direct physical interest to us.

Figure 5 shows $G(n, Q)$ as a function of n for $Q = D/S\alpha = 0.1$, 1.0, 10.0. The curve for the larger value of Q is higher. We recall that n represents the separation between two line-of-sight directions, measured in pixel widths. With these results in hand, we are now ready to consider their application to the type of question that is of interest here, as discussed in Section 1. A sample case is considered in Section 6.

6. APPLICATION OF RESULTS: PIXEL SEPARATION VARIATION STATISTICS

For an irregularity in the apparent height of the horizon line to suggest the presence of a target just above the horizon, it is necessary that the height irregularity occur within the span of 1 or at most 2 pixels' width. Using the results shown in Fig. 5, we can calculate the relevant statistics for the evaluation of the likelihood and/or the import of such an occurrence. A relevant sample case is one for which the sensor aperture diameter is $D = 0.15$ m, the propagation path length, i.e., the distance to the horizon, is $S = 1.5 \times 10^4$ m, and the sensor design is such that pixel angular size is $\alpha = 1 \times 10^{-4}$ rad. The strength of turbulence along the propagation path is considered to be of the order of $C_N^2 = 3 \times 10^{-14}$.

Examining the results in Fig. 5, we can see that for this small a span, i.e., for pixels with a horizontal separation of only $n \leq 1$ to 3 pixel widths, the value of $G(n, Q)$ is of the order of 2×10^{-3} for the ratio of sensor aperture diameter D to the source-pixel size $S\alpha$ equal to

$$Q = \frac{D}{S\alpha} = 0.1. \tag{44}$$

In this case for $n = 1$ to $n = 3$ we have $G(n, Q) \approx 1.7 \times 10^{-3}$ to $G(n, Q) \approx 2.0 \times 10^{-3}$. With $C_N{}^2 = 3 \times 10^{-14}$ m$^{-2/3}$ and Eq. (42) we calculate that

$$\begin{aligned}\mathcal{D}_{\Theta_y}(n, 0) &= 2.91\frac{256}{\pi}1.5 \times 10^4 (0.15)^{-1/3} 3 \times 10^{-14} \\ &\quad \times [0.0017 \text{ to } 0.0020]) \\ &= ([1.847 \times 10^{-5} \text{ to } 2.004 \times 10^{-5}] \text{ rad})^2 \\ &= ([0.1847 \text{ to } 0.2004]\alpha)^2. \end{aligned} \tag{45}$$

The physical implication of these values is that the image of the horizon line will manifest height irregularities of the order of 18% to 20% of a pixel's height.

Whether this represents a significant irregularity depends on the exact details of the engagement and of the signal processing and on the required detection and false-alarm probabilities. If, e.g., we require a false-alarm rate associated with a standard deviation level of 5, then we

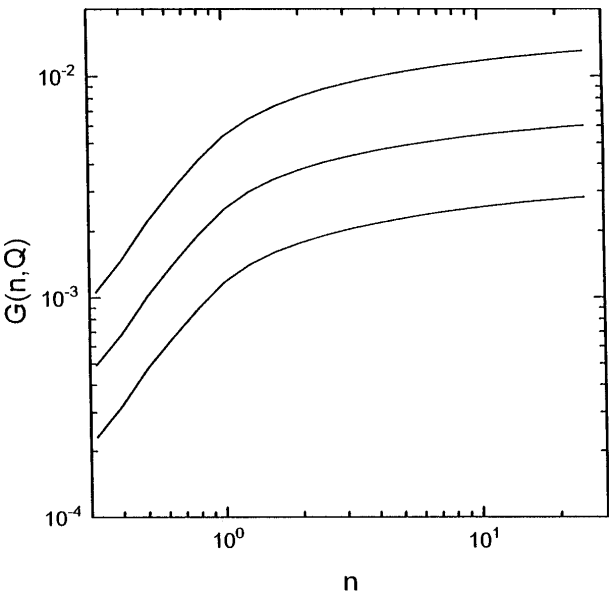

Fig. 5. $G(n, Q)$ versus n. The three curves correspond to $Q = D/(S\alpha) = 0.1$, 1.0, 10.0, respectively (the higher curve goes with the larger value of Q).

must consider that we have to accommodate a vertical displacement of approximately one pixel. If we are looking for an object that is nominally only 1 pixel above the nominal horizon, this much perturbation in the regularity of the image of the horizon line could prevent achievement of satisfactory performance if we intend to rely on the detection and/or the recognition of the presence of a manmade object just above the horizon by noting the presence of a 1-pixel-high bump in an only nominally smooth image of the horizon line.

REFERENCES AND NOTES

1. It has been pointed out by one of the reviewers that if we were to pay attention to the statistics of the difference of vertical displacements between pixels with a large horizontal separation, we would be studying a potentially miragelike phenomenon. However, I believe that in fact the results would indicate that the phenomenon is not particularly miragelike. This is because the turbulence statistics are random and vary reasonably rapidly, whereas the vertical refractive-index pattern that gives rise to the mirage effect is not random in the way turbulence is and does not vary rapidly as turbulence does. Nonetheless, the mirage phenomenon is also of potential concern as it, too, can produce effects that will interfere with detection of targets at the horizon. The interested reader may wish to refer to a general discussion of mirage effects such as is provided by A. B. Fraser and W. H. Mach, Sci. Am. **234**(1), 102–111 (1976).
2. D. L. Fried, "Turbulence-induced variation in the apparent separation of a pair of point sources," submitted to J. Opt. Soc. Am. A.